

Article

Multiresponse Performance Evaluation and Life Cycle Assessment for the Optimal Elimination of Pb (II) from Industrial Wastewater by Adsorption Using Vine Shoot Activated Carbon

Celia Sabando-Fraile, Marina Corral-Bobadilla *, Rubén Lostado-Lorza and Fátima Somovilla-Gomez

Department of Mechanical Engineering, University of La Rioja, 26004 Logroño, Spain; celia.sabando@unirioja.es (C.S.-F.); ruben.lostado@unirioja.es (R.L.-L.); fatima.somovilla@unirioja.es (F.S.-G.)
* Correspondence: marina.corral@unirioja.es; Tel.: +34-941-299-274

Abstract: Excess Pb (II) concentrations in wastewater have raised concerns of a risk to health and the environment due to their toxicity. This has contributed to the need for sustainable technology to remove heavy metals from wastewater. Biosorption provides a potential contribution to a solution. This study proposes a cost-effective method to remove lead ions from wastewater through the use of activated carbon from vine shoots as a biosorbent. However, economic cost and environmental impact are aspects that are necessary to study. This research suggests the use of a life cycle assessment and multiresponse surface method with desirability functions to improve and optimize the biosorption process. The experiments were conducted using a Box–Behnken design of experiments (BBD) combined with the multiresponse surface method. Three input variables were considered. They are initial lead concentration, pH, and the amount of activated carbon from vine shoots. These are the most significant adsorption process variables. The final lead concentration was considered as a process output variable. Human toxicity, global warming, abiotic depletion (fossil fuel), marine aquatic ecotoxicity, and freshwater ecotoxicity were regarded as process environmental impacts. Four optimization scenarios were proposed using these methods. The maximum removal of lead was 92.12%, whereas 92.09% of lead was removed when the minimum dose of vine shoot activated carbon was used. In contrast, 52.62% of lead was removed in the case of minimal environmental impact.

Keywords: biosorption; heavy metals; vine-shoot-derived activated carbon; wastewater; multiresponse surface methodology; life cycle assessment

Citation: Sabando-Fraile, C.; Corral-Bobadilla, M.; Lostado-Lorza, R.; Somovilla-Gomez, F. Multiresponse Performance Evaluation and Life Cycle Assessment for the Optimal Elimination of Pb (II) from Industrial Wastewater by Adsorption Using Vine Shoot Activated Carbon. *Sustainability* **2023**, *15*, 11007. <https://doi.org/10.3390/su151411007>

Academic Editor: Luca Di Palma

Received: 16 June 2023

Revised: 3 July 2023

Accepted: 10 July 2023

Published: 13 July 2023



Copyright: © 2023 by the authors. Licensee MDPI, Basel, Switzerland. This article is an open access article distributed under the terms and conditions of the Creative Commons Attribution (CC BY) license (<https://creativecommons.org/licenses/by/4.0/>).

1. Introduction

In recent decades, the release of heavy metals into water, such as lead, has increased remarkably due to industrial processes. The pollution that most affects the aquatic environment is produced by the discharge of heavy metals by industrial wastewater [1]. Depending on chemical species, their persistence, and their tendency to accumulate, there are several methods to remove them from industrial wastewaters. Due to the increase of Pb in several industrial activities and the increased use of products that contain it, including oil, agrochemicals, batteries, and paint, and the absence of natural pathways for the elimination of this pollutant, the food chain may become at risk of lead contamination and, hence, pose a risk to our drinking water and food [2]. This pollutant, which is the second-most-toxic metal, is a non-disintegrative heavy metal. It is highly noxious and exceedingly toxic to biological systems [3]. Pb toxicity can cause cognitive behavioral

problems, even at low concentrations. Additionally, Pb exposure worsens oxidative stress, causes neurological problems, alters sodium ion concentration, and can be fatal [4].

To decrease the levels of metals in water and wastewater, several techniques are available. These include ion exchange, membrane filtration [5,6], adsorption, chemical precipitation, ultrafiltration [7,8], electrochemical reactions, and improved oxidation techniques [9]. Newer, more efficient, more cost-effective, and inventive technologies have been the subject of increased research recently. Novel adsorbents have been introduced for improved adsorption. These include hydrogels [10,11], photocatalysis, electrodialysis, and membrane separation techniques [12,13], as well as magnetic nanoparticles [14]. However, there are significant downsides in using these approaches. These may entail high energy requirements, low effectiveness, inadequate elimination, expensive disposal methods, and one of the possible problematic working conditions. Because of its flexibility in designing and operating, as well as its effect on toxicity, heavy metal transport in wastewater, and biological availability, adsorption technology stands out from other technologies [15].

Due to the possibility of desorption (the opposite process), the adsorption is frequently reversible. In the latter case, adsorbate ions leave the surface of the adsorbent. This causes the process to be cost-effective and highly efficient in producing treated effluents of high quality [16]. Due to its ease of use, high capacity, and effectiveness in eliminating lead, even at very low lead concentrations, activated carbon emerges as one of the most efficient adsorbents [17].

The main by-product generated during the annual vegetative cycle of a vineyard are vine shoots, with a yield of between 2 and 4 tons per hectare (t/ha) [18]. The latest available data indicate that the amount of vine shoots generated during the 2021–2022 harvest campaign was approximately 260 kt. This reflects the high amount of waste generated in this sector annually. Considering the significance of the wine industry in the Autonomous Community of La Rioja and the volume of waste generated in wineries, the purpose of this paper is to research the use of activated carbon from vine shoots as an economically and environmentally viable alternative. This approach allows for the recovery of these by-products and contributes to the circular economy. In this work, the biosorption process uses activated carbon derived from vine shoots. However, to date, no studies have been conducted using vine shoot activated carbon for the removal of lead ions from wastewater. Other residues from agricultural production, from which activated carbon can be obtained, can be used as a sorbent. These include prickly pear seeds [19], banana peel [20], coconut shells [21], corncob [22], and black cumin [23]. The adsorption method used to remove Pb (II) from industrial wastewater with vine shoot activated carbon is typically affected by three process inputs or factors. They are the vine shoot activated carbon dose, the initial lead concentration, and the solution's pH. However, the variable or output to adjust is the amount of lead that remains in the wastewater after treatment.

Finding the input variables that provide the highest level of efficiency in the Pb (II) adsorption process is the objective of process optimization. One-variable-at-a-time experimentation is the conventional approach to this. However, in order to achieve the best results, this approach must be changed. The relationship between the several variables is not resolved by this technique, because the effect of these elements is complicated. So, this method is time and labor-intensive. Additionally, it requires a great deal of experimentation. As a result, the strategy is pricey. The use of multivariate statistical techniques enables the number of tests to be significantly reduced, as well as the descriptions of the effects of independent variables. This lowers the cost of trials greatly and aids the development of the operating system. Multiresponse surface (MRS) is an efficient and effective statistical technique for building regression models based on second-order polynomials. By considering only the most important elements, this model enhances the effectiveness of the process, while reducing the number of variables. This also reduces the cost and duration of experimentation [24].

Life cycle assessment (LCA) is a methodology to evaluate emissions and to determine the amount of raw materials and energy used, the quantity of waste produced, and their

effects during a product's life [25]. The net environmental implications of wastewater treatment methods and facilities have been thoroughly assessed using LCA and various alternative treatments. LCA can be used to analyze the environmental expense and benefit of removing pollutants to comply with stricter regulations. Its scope includes both indirect emissions that are attributable to the transport and production of chemicals and direct emissions from wastewater treatment plants, as well as the energy used and infrastructure necessary for treatment [26]. Most conducted research has been devoted to the study of the removal of nutrients. However, few studies have concentrated on the removal of pollutants of increasing concern, such as industrial and commercial chemicals. LCA, which takes into account the entire cycle of life of these activities, is an ideal technique for this study. It is necessary to overcome the negative contributions to prevent the initial problem's solution from being embroiled in further environmental problems [27]. Activated carbon (AC) is regarded as the best solution for the long term. It uses less power, although it has a lower removal efficiency than reverse osmosis and ozonation [28]. In addition, activated carbon is more suitable for the reuse of wastewater, because it has higher efficiency in the removal of heavy metals and also prevents the creation of toxic by-products during the treatment [29].

The objective of this work was to thoroughly investigate the optimization of the utilization of vine shoot AC as a biosorbent to reduce Pb (II) concentrations in industrial wastewater. Regression models were created based on the experimental results utilizing a Box–Behnken design (BBD) and MRS. They link the final Pb (II) ion concentration (C_f) to the input variables in the treated wastewater, vine shoot activated carbon (*dose*), initial lead concentration (C_0), and the solution's pH (pH). A multiobjective optimization was completed in this work using the MRS with desirability functions. The goal was to maximize the removal of Pb (II) and decrease the environmental impact and the dosage of vine shoot AC consumption of the biosorption process. In order to improve the development of Pb (II) removal technology for industrial wastewater, this work provides a mechanism that research and industry can use (Figure 1).

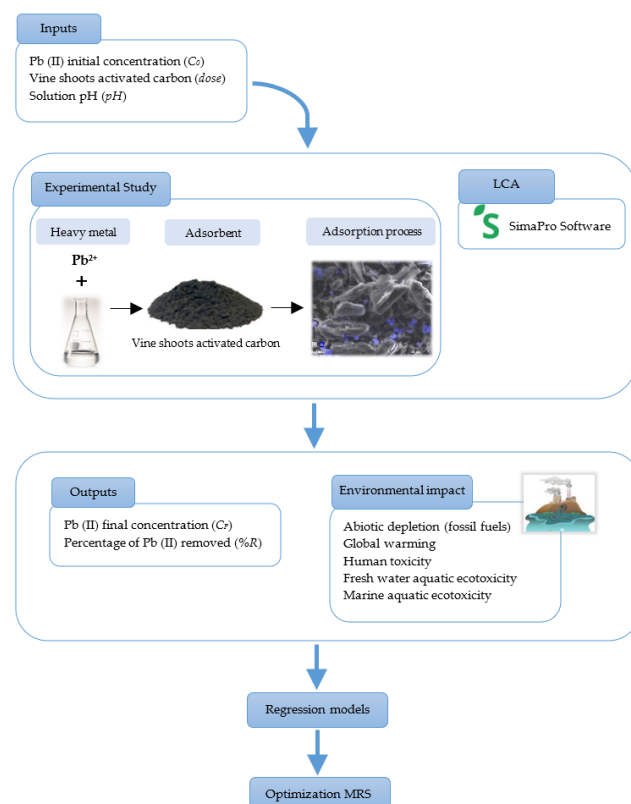


Figure 1. Methodological workflow.

2. Materials and Methods

2.1. Chemicals and Techniques

The method used in this work for the elimination of the heavy metal Pb (II) was adsorption, using vine shoot activated carbon as the biosorbent for the process. All procedures used reagents of analytical grade from Merck & Company (Darmstadt, Germany).

The vine shoots were collected from a vineyard in Cárdenas, La Rioja (Spain) following the harvest. The vine shoots were cleaned manually, dried for 24 h, and then chopped into small pieces that were soaked in a ZnCl₂ (98% extra-pure, CAS: 7646-85-7) solution for 24 h to chemically activate. Next, they were dried in an oven at 115 °C for 14 h and then carbonized at 800 °C in a nitrogen atmosphere. After that, they were soaked in HCl overnight at room temperature, filtered, and washed with deionized water until the pH reached neutrality. The final step in the production of the activated carbon was grinding with a high-speed grinder. This particular adsorbent was chosen because of its efficiency in the purification and removal of heavy metals. In addition, this adsorbent is an easy-to-reuse organic material that can be obtained from shredded vine shoots [30]. As a result of the large surface area of its microporous structure, as well as its complicated chemical composition and the variable functional groups on its exterior surface, activated carbon is often used as a biosorbent in water treatment facilities for the removal of metals. It has been shown that the pore size distribution and surface functional groups affect the biosorption efficiency of AC. Activated carbon may, however, interact with oxygen at temperatures of approximately 300 °C [31].

In this study, it was desirable that the lead adsorption capacity was not altered by the presence of other metals in the wastewater. Therefore, because it was not possible to obtain a real water sample, synthetic samples were prepared with deionized water and various initial Pb (II) concentrations of 8 to 30 ppm. To prepare the solution of 30 mg/L of lead required dissolving 0.056 g of PbCl₂·6H₂O (98% extra-pure, CAS 7758-95-4) in 1 L of distilled water. The pH adjustment process used an XS PH60 Violab DHS pH meter (Lab-process, Barcelona, Spain) following calibration with buffers at a pH of 4.0, 7.0, and 10.0, according to the ASTM D1293-18 standard [32].

2.2. Response Surface Method for Pb Adsorption Process

The response surface method (RSM) approach was used to establish relationships between the input parameters of the Pb adsorption process and output variables. The input parameters studied were activated carbon dose (*dose*), initial lead concentration (*C*₀), and pH (*pH*). The output variables were the final lead concentration in treated wastewater (*C*_f) and the percentage of ions of lead that were present in the treated wastewater (%*R*). In 1951, Box and Wilson released the RSM [33], enabling experimental data to be utilized for models or the best possible responses. The approach was initially created to simulate experimental results. However, it helps with product and industrial process optimization. In addition, it can be used to model the optimal elimination of heavy metals [34,35] using experimental data. A Box–Behnken design of experiments (BBD) [36] was used to fit a second-order polynomial model using a low-degree polynomial regression model, as shown in the following Equation (1):

$$A = f(B_1, B_2, B_3, \dots, B_k) + e \quad (1)$$

The polynomial has the following components: *A* is the predicted output or experimental response; *f* is a cross product of the components of the polynomial; *B*₁, *B*₂, *B*₃, ..., *B*_{*k*} represent the input process parameters; and *e* refers to the error. Polynomial functions are often used. A quadratic (second-order) model is one of them. This may be seen below in Equation (2):

$$A = c_0 + \sum_{i=1}^m c_i \cdot B_i + \sum_{i=1}^m c_{ii} \cdot B_i^2 + \sum_{i=1}^{m-1} \sum_{j=i+1}^m b_{ij} \cdot B_i \cdot B_j + e \quad (2)$$

The values of the c_0 , c_i , c_{ii} , and c_{ij} coefficients were determined using regression analysis. However, when dealing with complicated situations with numerous inputs and nonlinearities, these functions may not always produce satisfactory solutions.

If the model yields accurate findings, the p -value (Prob. > F) indicates the probability that the outcome will not be smaller than what was observed. By making use of an N analysis of variance (ANOVA), the p -value may be determined. The model's output will be acceptable with a $(1 - \alpha)$ confidence interval if it exceeds that for model F. No model terms have a significance level (e.g., $\alpha = 0.05$) above them. The ideal configuration of outputs may differ greatly from one another. This implies that there are competing outputs. Harrington created the desirability function [37]. It includes an overall desirability and desirability functions for each output variable as seen in Equations (3) and (4). The latter represents the arithmetic mean of each output's desirability (D) value using Equation (5).

$$d_r^{\max} = \begin{cases} 0 & \text{if } f_r(B) < C \\ \left(\frac{f_r(B)-G}{B-G}\right)^S & \text{if } C \leq f_r(B) \leq G \\ 1 & \text{if } f_r(B) > G \end{cases} \quad (3)$$

$$d_r^{\min} = \begin{cases} 1 & \text{if } f_r(B) < C \\ \left(\frac{f_r(B)-G}{C-G}\right)^S & \text{if } C \leq f_r(B) \leq G \\ 0 & \text{if } f_r(B) > G \end{cases} \quad (4)$$

$$D = \left(\prod_{r=1}^R d_r \right)^{1/R} \quad (5)$$

where B is the input vector; C and G have the lowest and highest values found for the response r and weight S. The use of a second higher-degree polynomial helps to optimize the replies [38].

2.3. Experiments Design

The design of experiments (DoE) is usually employed in building precise models with the fewest data required to validate the original hypothesis [39,40]. A design matrix (of inputs) may be produced using any of the several available methodologies to measure the outputs or responses. The experiment in this instance was created through the use of a BBD. The input parameters chosen to create the DoE were, as previously noted: vine shoot activated carbon dose (*dose*), initial lead concentration (C_0), and solution pH (*pH*). The variables from each experiment that were selected for optimization are listed in Table 1 (design matrix) along with their relevant ranges and levels.

Table 1. Design matrix: biosorption process inputs and levels considered.

Input	Notation	Magnitude	Levels		
			-1	0	1
Initial Pb (II) concentration	C_0	mg/L	8	19	30
Vine shoot activated carbon dose	<i>dose</i>	G	1.6	3.8	6
pH	<i>pH</i>	-	2.8	5	7.2

The design matrix was generated using R Statistical Software v.1.6 [41] after the biosorption process's characteristics. A total of 17 experiments were conducted in order to ensure that all potential Pb (II) adsorption process input parameters were considered and

a regression model was obtained that would determine the most relevant inputs for the ion Pb (II) adsorption process.

2.4. Life Cycle Assessment (LCA)

ISO 14040/14044 [42] establishes the life cycle assessment and also addresses the impact of actions on the environment [39,40]. Examples include using the resources and impact of emissions on the environment during the laboratory trials of the adsorption of lead by vine shoot activated carbon. An LCA study has four phases. The first involves the scope of the study and definition. The remaining three phases address inventory analysis, environmental impact assessment, and interpretation. In this case, the method that is known as gate-to-gate was used. This is the process of determining the variables that probably had the most environmental impact using scaled-up inventory data. The wastewater samples were prepared in the laboratory, as shown in Tables 1 and 2. In order to conduct the LCA quantitatively, every training test considered the initial and final lead concentrations in water, the dosage of vine shoot activated carbon, and the dosage of H₂SO₄ and NaOH used to modify the water pH. There were three values for the input parameter of pH: 2.8, 5, and 7.2. The initial solution pH was 5.8 as distilled water was used. Thus, it was necessary to add a certain amount of H₂SO₄ to lower the pH to values of 2.8 and 5 and to calculate the amount of NaOH to increase the pH to 7.2 (see Table 2).

Table 2. H₂SO₄ and NaOH concentrations to modify the water's pH.

pH	Dose of H ₂ SO ₄ [g]	Dose of NaOH [g]
2.8	0.0505	-
5	8.0062	-
7.2	-	1.5924

Table 3 shows the items considered for the environmental inventory. This study is referred to as gate-to-gate. It generated the environmental inventory using scaled-up inventory data from the Ecoinvent 3 database, which provided the inventory information for the input parameters of the adsorption process, as well as for all human-activity-related economic activities [43]. This involved the use of vine shoot activated carbon to remove an initial lead concentration from one liter of deionized water and sulfuric acid or sodium hydroxide to modify the water's pH. After this adsorption process, the treated water still contained lead that the process had not removed.

Table 3. Inventory information utilized for Simapro calculations.

Item	Unit	Material
Output	mg	Initial Pb (II) concentration
Output (removed products)	mg	Removed lead
Input (resources)	L	Water
Input (materials/fuels)	g	Vine shoot activated carbon Sulfuric acid Sodium hydroxide
Water emissions	mg	Final Pb (II) concentration

In this work, the information was processed using Simapro® v.9.2.0.2 software. The LCA was based on the CML-IA baseline V3.06/EU25 approach. The LCA is limited to the initial phases of the cause–effect chain as part of the CML-IA baseline impact assessment procedure in order to reduce uncertainty. The latter were categorized in the middle and included human toxicity, eutrophication, abiotic depletion (fossil fuels), global warming, freshwater ecotoxicity, and marine aquatic ecotoxicity. This study did not consider the other environmental effects. These included terrestrial ecotoxicity, photochemical

oxidation, abiotic depletion and ozone layer depletion, eutrophication, or acidification. Their environmental impact is significantly less than that of the elements that were considered. The University of Leiden in the Netherlands [44] developed this impact assessment, which is used extensively throughout Europe. The IPCC, the International Panel on Climate Change, has issued a warning about factors that are involved in the production and/or distribution of greenhouse gases (GHGs), as well as a 100-year time horizon for action in kg CO₂ eq. These factors were used to evaluate the implications of climate change [45]. The effects on human toxicity and freshwater ecotoxicity were evaluated using the consensus technique USEtox [46]. The measure of the potential harm to humans due to the discharge of chemicals into the environment is known as human toxicity. It indicates the possible lead concentration, as well as its innate toxicity [47]. The scope of lead removal from wastewater using vine shoot activated carbon for the biosorption process covered gate to gate in the current research.

2.5. Pb (II) Adsorption Experiments

Laboratory experiments were conducted using the BBD design matrix. Each experiment served to establish the sorption process for the efficient reduction of lead ions. The adsorbent was separated by filtering with 0.25 µm filters. The test samples were gathered, placed into glass bottles, and analyzed for residual Pb (II) using a Unicam-929 atomic adsorption spectrophotometer (Unicam Ltd., Cambridge, UK). Equation (6) uses the data from C_F and C_0 to calculate the removal efficiency (%R).

$$\%R = \frac{C_0 - C_F}{C_0} \cdot 100 \quad (6)$$

2.6. Scanning Electron Microscopy (SEM) and Energy-Dispersive X-ray (EDX) Characterization

A model S-2400 Hitachi (Osaka, Japan) scanning electron microscope examined at an operating voltage of 18 kV the surfaces of samples of the vine shoot activated carbon. The operating voltage that was employed was 18 KV. The samples were first coated with a 1 nm layer of gold–palladium to ensure conductivity by plasma sputtering for 60 s. Following lead biosorption, SEM micrographs of the vine shoot activated carbon revealed the surface texture to be flocced and porous. In addition, the biocarbon from grape stalk waste contained lead ions on its surface.

The elemental composition of the activated carbon in vine shoots was qualitatively analyzed using an EDX (energy-dispersive X-ray) Quantax 200 spectroscope (Bruker, Billerica, MA, USA), along with ESPRIT 1.9 microanalysis software and an XFlash 5010/30 detector.

3. Results and Discussion

3.1. Experimental Results

The final Pb (II) concentration (C_F) was established experimentally after the input parameters for the adsorption process from the DoE had been set. In conformity with the Box–Behnken DoE's design matrix, Table 4 provides the experimental findings for the output variable (C_F). They represent the final Pb (II) ion concentration of the treated wastewater. By using Equation (6), the percentage of lead that was removed (%R) during the biosorption process can be calculated.

Table 4. Experimental results for the output variables.

Sample	Input Parameters			Output Parameters	
	C_0	Dose	pH	C_F	%R
1	8.0	3.8	2.8	1.83	77.14
2	19.0	1.6	2.8	10.58	44.33
3	19.0	6.0	2.8	5.30	72.11
4	30.0	3.8	2.8	8.59	71.37
5	30.0	1.6	5.0	16.97	43.44
6	19.0	3.8	5.0	10.15	46.6
7	19.0	3.8	5.0	7.06	62.83
8	8.0	1.6	5.0	2.00	75.06
9	19.0	3.8	5.0	6.12	67.78
10	19.0	3.8	5.0	6.34	66.62
11	30.0	6.0	5.0	13.39	55.37
12	19.0	3.8	5.0	7.25	61.85
13	8.0	6.0	5.0	4.54	43.26
14	8.0	3.8	7.2	2.32	71.02
15	30.0	3.8	7.2	5.45	81.85
16	19.0	1.6	7.2	2.52	86.73
17	19.0	6.0	7.2	9.51	49.97

The 17 samples or adsorption processes were completed in accordance with the BBD design matrix. The output process variables were then computed in the lab. Simapro® v.9.2.0.2 software, in compliance with CML-IA baseline V3.06/EU25, was used to calculate the effect of the process on the environment. These results appear in Table 5.

Table 5. Results for the environmental impact category.

Sample	Impact Category				
	Abiotic Depletion (Fossil Fuels) (MJ)	Global Warming (GWP100a) (kg CO ₂ eq.)	Human Toxicity (kg 1.4 DB eq.)	Freshwater Ecotoxicity (kg 1.4 DB eq.)	Marine Aquatic Ecotoxicity (kg 1.4 DB eq.)
1	0.14031	0.01245	0.00465	0.00397	14.68094
2	0.10714	0.00651	0.00475	0.00331	11.10334
3	0.18840	0.01374	0.00740	0.00557	19.64768
4	0.05909	0.00523	0.00204	0.00173	6.15660
5	0.18507	0.01660	0.00911	0.00713	22.47006
6	0.18832	0.01373	0.00734	0.00552	19.61565
7	0.10733	0.00653	0.00462	0.00321	11.15192
8	0.18456	0.01655	0.00899	0.00704	22.29842
9	0.18829	0.01373	0.00732	0.00550	19.60588
10	0.18830	0.01373	0.00732	0.00551	19.60817
11	0.22125	0.01964	0.00733	0.00625	23.12808
12	0.26934	0.02093	0.01008	0.00785	28.09246
13	0.26934	0.02093	0.01008	0.00785	28.09246
14	0.18832	0.01373	0.00734	0.00552	19.61758
15	0.26970	0.02096	0.01008	0.00785	28.20465
16	0.26612	0.02381	0.01187	0.00948	30.95582
17	0.13989	0.01241	0.00461	0.00394	14.54704

3.2. Analysis of Variance

Equation (2) was adjusted with the results that appear in Tables 4 and 5, in order for the R Statistical Software to produce regression equations for the answers [41]. For every response, a second-order polynomial model was constructed. The most accurate model was then selected by considering a variety of variables, such as the p -value, RMSE, MAE, and correlation. Equations (7)–(12) gave second-degree polynomial functions for modeling the final Pb (II) concentration (C_f) and the following environmental impacts: abiotic depletion (Ab_depl) and global warming (Gl_War), human toxicity ($Hum_along\ with\ Tox$), freshwater ecotoxicity ($Fresh_W$), and marine aquatic ecotoxicity (Mar_Aqu).

$$C_f = 2.25846 + 2.50972 \cdot pH - 0.52862 \cdot pH^2 + 0.62343 \cdot C_0 - 5.25445 \cdot dose + 0.6334 \cdot pH \cdot dose - 0.06325 \cdot C_0 \cdot dose + 0.43782 \cdot dose^2 \quad (7)$$

$$Ab_depl = -0.1795676 + 0.0520377 \cdot pH + 0.0065755 \cdot C_0 - 0.0001735 \cdot C_0^2 + 0.0379922 \cdot dose - 0.0085424 \cdot pH \cdot dose + 0.0042358 \cdot dose^2 \quad (8)$$

$$Gl_War = -0.00591018 + 0.00039723 \cdot pH^2 + 0.00044878 \cdot C_0 - 1.185 \times 10^{-5} \cdot C_0^2 + 0.00342053 \cdot dose - 0.00062016 \cdot pH \cdot dose + 0.00030288 \cdot dose^2 \quad (9)$$

$$Hum_Tox = -0.005933866 + 0.001904029 \cdot pH + 0.000149535 \cdot C_0 - 3.944 \times 10^{-6} \cdot C_0^2 + 0.001114101 \cdot dose - 0.000180785 \cdot pH \cdot dose + 0.000105943 \cdot dose^2 \quad (10)$$

$$Fresh_W = -0.002975238 + 0.000660279 \cdot pH + 7.939 \times 10^{-5} \cdot pH^2 + 0.000121702 \cdot C_0 - 3.209 \times 10^{-6} \cdot C_0^2 + 0.000959081 \cdot dose - 0.000149277 \cdot pH \cdot dose + 8.6622 \times 10^{-5} \cdot dose^2 \quad (11)$$

$$Mar_Aqu = -18.08497 + 5.34325 \cdot pH + 0.54355 \cdot C_0 - 0.01444 \cdot C_0^2 + 3.82106 \cdot dose - 0.72873 \cdot pH \cdot dose + 0.37944 \cdot dose^2 \quad (12)$$

In addition, Tables 6–11 provide the ANOVA results for the quadratic models that were developed, along with a determination of whether any interactions or other effects were statistically significant and had a p -value ($Pr(>F)$). These tables show that most of the input variables' p -values and their combinations were lower than 0.05. Table 6 shows that the analysis of variance results support the conclusion that the initial lead concentration (C_0) (p -value = 0.00030) directly influenced the output parameter of the final lead concentration (C_f). In contrast, the other input parameters, solution pH (pH) (p -value = 0.30083) and dose of vine shoot activated carbon ($dose$) (p -value = 0.91229), had no significant influence. However, they did when combined to create what are known as interaction effects ($pH \cdot dose$) with a p -value of 0.01684. Furthermore, the pH (pH) had a significant effect when it was squared (pH^2) (p -value = 0.04003). Due to this disparity in the results for the p -values of pH, which directly affect the final concentration, it is proposed that the dependence of these two variables be verified by the second-degree polynomial equation that was obtained (Equation (7)). Therefore, Figure 2 shows the effect of the solution pH on Pb (II) biosorption at various initial lead concentrations (8, 19, and 30 ppm) and for different vine shoot activated carbon dosages (1.6 and 6 g). Figure 2a shows that, at a low biosorbent dose ($dose = 1.6$ g), the minimum final Pb (II) concentration was reached at a low initial lead concentration ($C_0 = 8$ ppm) and a high solution pH ($pH = 7.2$). Additionally, the maximum final Pb (II) concentration was reached at a high initial concentration ($C_0 = 30$ ppm) and low solution pH ($pH = 2.8$). However, Figure 2b shows the opposite. It shows that with a high biosorbent dose ($dose = 6$ g), the minimum final Pb (II) concentration was reached at a low initial lead concentration ($C_0 = 8$ ppm) and a low solution pH ($pH = 2.8$). Additionally, it shows that the maximum final Pb (II) concentration was reached at a high initial concentration ($C_0 = 30$ ppm) and a high solution pH ($pH = 7.2$). Thus, it can be concluded that the final lead concentration depends on the pH of the solutions, as stated in other references related to lead removal using activated carbon [48,49] and vine shoot activated carbon [50,51].

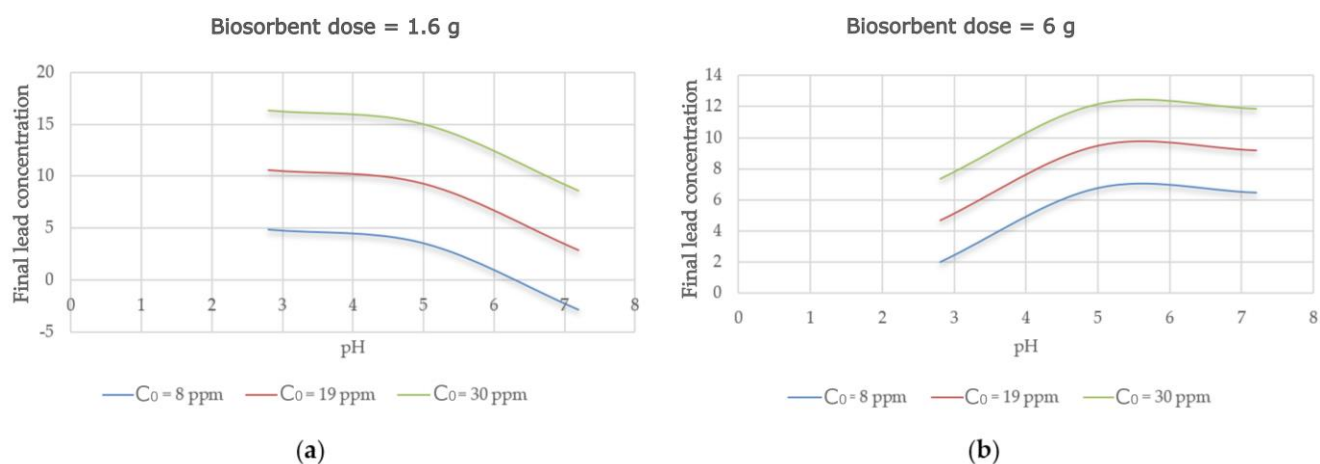


Figure 2. Variation of final lead concentration vs. pH for different values of C_0 when: (a) dose = 1.6 g, (b) dose = 6 g.

Table 6. Results of analysis of variance values for the C_F quadratic model.

Variable	Df	Sum of Sq	Mean Sq	F Value	Pr (>F)
pH	1	5.28743	5.28743	1.20497	0.30083
pH^2	1	25.23138	25.23138	5.75008	0.04003
C_0	1	142.04046	142.04046	32.37014	0.00030
dose	1	0.05631	0.05631	0.01283	0.91229
$pH \cdot dose$	1	37.59284	37.59284	8.56718	0.01684
$C_0 \cdot dose$	1	9.37278	9.37278	2.13600	0.17789
$dose^2$	1	18.95926	18.95926	4.32070	0.06741
Residuals	9	39.49208	4.38801		

Table 7. Results of analysis of variance values for the Ab_{depl} quadratic model.

Variable	Df	Sum Sq	Mean Sq	F Value	Pr (>F)
pH	1	0.01484	0.01484	21.28288	0.00096
C_0	1	2.738×10^{-7}	2.738×10^{-7}	0.00039	0.98458
C_0^2	1	0.00167	0.00167	2.39403	0.15284
dose	1	0.02922	0.02922	41.91184	0.00007
$pH \cdot dose$	1	0.00684	0.00684	9.80667	0.01066
$dose^2$	1	0.00177	0.00177	2.54513	0.14172
Residuals	10	0.00697	0.00070		

Table 8. Results of analysis of variance values for the GI_{War} quadratic model.

Variable	Df	Sum Sq	Mean Sq	F Value	Pr (>F)
pH^2	1	0.00011	0.00011	32.84643	0.00019
C_0	1	2.450×10^{-9}	2.450×10^{-9}	0.00072	0.97908
C_0^2	1	7.058×10^{-6}	7.058×10^{-6}	2.08162	0.17966
dose	1	0.00027	0.00027	78.48563	4.767×10^{-6}
$pH \cdot dose$	1	4.212×10^{-5}	4.212×10^{-5}	12.42308	0.00550
$dose^2$	1	9.069×10^{-6}	9.069×10^{-6}	2.67487	0.13299
Residuals	10	3.391×10^{-5}	3.391×10^{-6}		

Table 9. Results of analysis of variance values for the *Hum_Tox* quadratic model.

Variable	Df	Sum Sq	Mean Sq	F Value	Pr (>F)
<i>pH</i>	1	5.7352×10^{-5}	5.7352×10^{-5}	164.192311	1.5726×10^{-7}
C_0	1	1.125×10^{-10}	1.125×10^{-10}	0.00032	0.98603
C_0^2	1	8.529×10^{-7}	8.529×10^{-7}	2.44172	0.14921
<i>dose</i>	1	3.992×10^{-5}	3.992×10^{-5}	114.27809	8.595×10^{-7}
<i>pH</i> · <i>dose</i>	1	3.063×10^{-6}	3.063×10^{-6}	8.76758	0.01426
<i>dose</i> ²	1	1.110×10^{-6}	1.110×10^{-6}	3.17818	0.10496
Residuals	10	3.493×10^{-6}	3.493×10^{-7}		

Table 10. Results of analysis of variance values for the *Fresh_W* quadratic model.

Variable	Df	Sum Sq	Mean Sq	F Value	Pr (>F)
<i>pH</i>	1	3.0459×10^{-5}	3.0459×10^{-5}	116.478307	1.89×10^{-6}
<i>pH</i> ²	1	6.310×10^{-7}	6.310×10^{-7}	2.41282	0.15476
C_0	1	5.000×10^{-11}	5.000×10^{-11}	0.00019	0.98927
C_0^2	1	5.662×10^{-7}	5.662×10^{-7}	2.16506	0.17526
<i>dose</i>	1	2.938×10^{-5}	2.938×10^{-5}	112.33719	2.200×10^{-6}
<i>pH</i> · <i>dose</i>	1	2.088×10^{-6}	2.088×10^{-6}	7.98482	0.01986
<i>dose</i> ²	1	7.401×10^{-7}	7.401×10^{-7}	2.83017	0.12680
Residuals	9	2.353×10^{-6}	2.615×10^{-7}		

Table 11. Results of analysis of variance values for the *Mar_Aqu* quadratic model.

Variable	Df	Sum Sq	Mean Sq	F Value	Pr (>F)
<i>pH</i>	1	256.557685	256.557685	48.988636	3.7192×10^{-5}
C_0	1	0.02718	0.02718	0.00519	0.94399
C_0^2	1	11.46931	11.46931	2.19002	0.16971
<i>dose</i>	1	362.83722	362.83722	69.28228	8.306×10^{-6}
<i>pH</i> · <i>dose</i>	1	49.75976	49.75976	9.50142	0.01159
<i>dose</i> ²	1	14.24024	14.24024	2.71912	0.13017
Residuals	10	52.37086	5.23709		

However, the dose of activated carbon (*dose*) had no significant effect when it was squared (*dose*²) (*p*-value = 0.06741) or combined with the initial concentration of lead (*C*₀·*dose*) (*p*-value = 0.17789). In short, the input variable that had the most influence on the output variable (i.e., *C*_F) was the initial concentration of Pb (II) (*C*₀). That is, the final lead concentration depended mainly on the initial lead concentration contained in the solution. The input variable that influenced the final lead concentration (*C*_F) the least was the dose of activated carbon (*dose*). This may be due to the fact that, if there is a saturation of vine shoot activated carbon, no further adsorption will occur during the process.

Tables 7–11 show that the input parameters of pH (*pH*) and dose of vine shoot activated carbon (*dose*) directly affected the effect of the process on the environment, except in the case of global warming (*Gl_War*). In this case, in Equation (12), the dose of vine shoot activated carbon just appeared squared. The initial lead concentration (*C*₀) had no significant effect. There were very similar results for the remaining output parameters of approximately 0.98. Table 7 shows that, for abiotic depletion (*Ab_depl*), the dose of activated carbon (*dose*) was the most significant variable (*p*-value = 0.00007), followed by pH (*p*-value = 0.00096). This was not true when it was squared (*dose*²) (*p*-value = 0.14172). The initial lead concentration (*C*₀) was the least significant variable (*p*-value = 0.98458). Additionally, it was not a significant variable when squared (*C*₀²) (*p*-value = 0.15284). For the environmental impact outputs, there was only one combination of the input variables. It was formed by the dose of activated carbon (*dose*) and the pH. In this case, for abiotic

depletion (*Ab_depl*), this combination (*pH·dose*) had a significant influence (p -value = 0.01066). In a similar fashion, Table 8 shows that the dose of activated carbon (*dose*) directly influenced the output variable of global warming (*Gl_War*) (p -value = 4.767×10^{-6}), as did the combination of input variables of pH squared (pH^2) (p -value = 0.00019) and pH with the dose of activated carbon ($pH \cdot dose$) (p -value = 0.00550). However, the initial lead concentration (C_0) had no significant influence (p -value = 0.97908), even if it was squared (C_0^2) (p -value = 0.17966). Similarly, Table 9 shows that, for human toxicity (*Hum_Tox*), the pH and the dose of activated carbon (*dose*) had a significant influence (p -value = 1.5726×10^{-7} and p -value = 8.595×10^{-7} , respectively). They also influenced human toxicity when they were combined ($pH \cdot dose$) (p -value = 0.01426). Nevertheless, the initial lead concentration (C_0), its square (C_0^2), and the square of dose of activated carbon ($dose^2$) had no influence (p -value = 0.98603, p -value = 0.14921, and p -value = 0.10496, respectively). Table 10 shows that, for freshwater ecotoxicity (*Fresh_W*), the pH (*pH*) and dose of activated carbon (*dose*) were the most significant variables (p -value = 1.89×10^{-6} and p -value = 2.200×10^{-6} , respectively), just as the combination of both input variables ($pH \cdot dose$) (p -value = 0.01986) was. Furthermore, the remaining input parameters had no influence on this environmental impact; the initial lead concentration (C_0) had a p -value = 0.98927 even if it was squared (C_0^2) (p -value = 0.17526), with other parameters as follows: (pH^2) (p -value = 0.15476) and ($dose^2$) (p -value = 0.12680). Finally, Table 11 shows that the pH (*pH*) and the dose of activated carbon directly influenced the environmental impact output of marine aquatic ecotoxicity (*Mar_Aqu*), with p -values of 3.7192×10^{-5} and 8.306×10^{-6} , respectively, as did the combination of both ($pH \cdot dose$) (p -value = 0.01159). However, the initial lead concentration (C_0), its square (C_0^2), and the square of the remaining input variable dose of activated carbon ($dose^2$) did not, with p -values of 0.94399, 0.16971, and 0.13017, respectively.

The interaction effects, square effects, and main effects of the process inputs were considered in this study to be significant second-order regression model variables. The analysis of the ANOVA results show that the second-order models' input process variables had statistically significant values. Additionally, we can also deduce from the analysis of variance that the input variables of pH (*pH*) and the dose of vine shoot activated carbon (*dose*) directly influenced the environmental impact of the sorption process. It is clear that this occurred because the LCA for the biosorption process in this research was covered gate-to-gate. Thus, neither the creation of activated carbon nor the subsequent treatments of the water emissions were considered in this work.

In line with Equations (7)–(12) and using the samples in Tables 6–11, we used the MAE and the RMSE to determine the generalization capability of the quadratic models.

$$MAE = \frac{1}{n} \cdot \sum_{i=1}^n |X_{i \text{ Test}} - X_{i \text{ Model}}| \quad (13)$$

$$RMSE = \sqrt{\frac{1}{n} \cdot \sum_{i=1}^n (X_{i \text{ Test}} - X_{i \text{ Model}})^2} \quad (14)$$

In this instance, the quadratic models that the RSM and n experiments developed are denoted by $X_{i \text{ Model}}$, whereas the empirically observed outputs are denoted by $X_{i \text{ Test}}$. The correlation and predicted errors are shown in Table 12. One can see that the correlation coefficients almost reached 100%. This indicates that the approximation of the theoretical model, predicted by the quadratic regression models, to the experimentally derived values is very good. Environmental impacts had the highest correlation values, with the best result in the case of human toxicity (*Hum_Tox*) (correlation = 98.335%), followed by the impact of freshwater ecotoxicity (*Fresh_W*) (correlation = 98.207%). The lowest correlation corresponded to the final Pb (II) concentration (C_F) (correlation = 92.626%). The reason for this is that the C_F was determined experimentally using a spectrophotometer and the environmental effects using software (Simapro®), which provided reliable correlation values. All of the variables that were examined also had very low MAE and RMSE values.

This shows that the quadratic regression models properly reflect the experimental findings and have a high degree of generalizability. Similar to the analysis of correlation, it can be noted that, for the values that the RMSE and MAE provided, the final lead concentration was the output variable that had the highest MAE and RMSE (7.948% and 10.068%, respectively). In contrast, the lower MAE and RMSE were associated with human toxicity (*Hum_Tox*) and freshwater ecotoxicity (*Fresh_W*), whereas the MAE and RMSE were 3.426% and 4.611% for the first variable and 3.565% and 4.801% for the second variable, respectively.

Table 12. Results of *p*-value, correlation, and errors in the output variables using the quadratic regression models.

	<i>p</i> -Value	Correlation	MAE Train	RMSE Train
C_F	$3.267E \times 10^{-3}$	92.6260%	7.9480%	10.0680%
<i>Ab_depl</i>	3.273×10^{-4}	94.1430%	7.3940%	9.6160%
<i>Gl_War</i>	3.639×10^{-5}	96.3230%	5.8890%	7.6010%
<i>Hum_Tox</i>	7.795×10^{-7}	98.3350%	3.4260%	4.6110%
<i>Fresh_W</i>	8.099×10^{-6}	98.2070%	3.5650%	4.8010%
<i>Mar_Aqu</i>	3.148×10^{-5}	96.4320%	5.5540%	7.0780%

3.3. Multiresponse Optimization

The optimal process variables within the required operating range were predicted using the desirability function tool in the R Statistical Software [41]. By using the desirability function, it is possible to maximize many replies. As a result, a projected response becomes a scale-free value response with an optimal value that ranges from the lowest to the optimal (from 0 to 1) [52]. Tables 13–16 provide the optimum results for the Pb (II) biosorption process in wastewater using activated carbon and MRS, which combined input and output parameters for four different optimization scenarios. These four scenarios reflect a tendency to minimize the final Pb (II) concentration in wastewater, the adsorbent dosage consumption, and the impact of the biosorption process on the environment. In this work, the input and output are both listed in the first column of each table. The goal is provided in the second column. The minimums and maximums (range) that were chosen for the adsorption optimization procedure appear in the third and fourth columns. The optimized values that were produced within the foregoing minimums and maximums are shown in the fifth column. The desirability values appear in the sixth column. The overall desirability was obtained from the maximization of individual desirability. It indicates how close a response is to the ideal value. If the desired value is reached, the coefficient will be equal to a single unit and will be nil otherwise.

Table 13. First adsorption optimization scenario: minimizing the final Pb (II) concentration.

	Goal	Minimum	Maximum	Optimum	Desirability
<i>pH</i>	inRange	2.80	7.20	7.00	1.000
C_0	inRange	8.00	30.00	14.14	1.000
<i>dose</i>	inRange	1.60	6.00	1.62	1.000
C_F	minimum	1.83	16.97	1.11	1.000
<i>Ab_depl</i>	inRange	0.0591	0.2697	0.2188	1.000
<i>Gl_War</i>	inRange	0.0052	0.0238	0.0168	1.000
<i>Hum_Tox</i>	inRange	0.0020	0.0119	0.0088	1.000
<i>Fresh_W</i>	inRange	0.0017	0.0095	0.0067	1.000
<i>Mar_Aqu</i>	inRange	6.16	30.96	23.04	1.000
Overall desirability					1.000

Table 14. Second adsorption optimization scenario: minimizing the vine shoot adsorbent dose to obtain the highest removal of Pb (II).

	Goal	Minimum	Maximum	Optimum	Desirability
<i>pH</i>	inRange	2.80	7.20	7.00	1.000
<i>C₀</i>	inRange	8.00	30.00	14.14	1.000
<i>dose</i>	minimum	1.60	6.00	1.60	1.000
<i>C_F</i>	minimum	1.83	16.97	1.12	1.000
<i>Ab_depl</i>	inRange	0.0591	0.2697	0.2189	1.000
<i>Gl_War</i>	inRange	0.0052	0.0238	0.0168	1.000
<i>Hum_Tox</i>	inRange	0.0020	0.0119	0.0088	1.000
<i>Fresh_W</i>	inRange	0.0017	0.0095	0.0067	1.000
<i>Mar_Aqu</i>	inRange	6.16	30.96	23.04	1.000
Overall desirability					1.000

Table 15. Third adsorption optimization scenario: minimizing the environmental impact to obtain the highest removal of Pb (II).

	Goal	Minimum	Maximum	Optimum	Desirability
<i>pH</i>	inRange	2.80	7.20	2.80	1.000
<i>C₀</i>	inRange	8.00	30.00	8.02	1.000
<i>dose</i>	inRange	1.60	6.00	2.05	1.000
<i>C_F</i>	minimum	1.83	16.97	3.80	0.757
<i>Ab_depl</i>	minimum	0.0591	0.2697	0.0545	1.000
<i>Gl_War</i>	minimum	0.0052	0.0238	0.0048	1.000
<i>Hum_Tox</i>	minimum	0.0020	0.0119	0.0020	1.000
<i>Fresh_W</i>	minimum	0.0017	0.0095	0.0017	0.997
<i>Mar_Aqu</i>	minimum	6.16	30.96	5.56	1.000
Overall desirability					0.954

Table 16. Fourth adsorption optimization scenario: minimizing the environmental impact and the adsorbent dose to obtain the highest removal of Pb (II).

	Goal	Minimum	Maximum	Optimum	Desirability
<i>pH</i>	inRange	2.80	7.20	2.80	1.000
<i>C₀</i>	inRange	8.00	30.00	8.01	1.000
<i>dose</i>	minimum	1.60	6.00	1.60	0.998
<i>C_F</i>	minimum	1.83	16.97	4.87	0.639
<i>Ab_depl</i>	minimum	0.0591	0.2697	0.0413	1.000
<i>Gl_War</i>	minimum	0.0052	0.0238	0.0035	1.000
<i>Hum_Tox</i>	minimum	0.0020	0.0119	0.0016	1.000
<i>Fresh_W</i>	minimum	0.0017	0.0095	0.0014	1.000
<i>Mar_Aqu</i>	minimum	6.16	30.96	4.15	1.000
Overall desirability					0.938

Table 13 shows the first optimization scenario, in which the goal is to obtain the minimum final lead concentration, while the remaining variables are in range. The second optimization scenario is provided in Table 14. This scenario involves the minimum vine shoot activated carbon dosage consumption. Thus, it minimizes the costs of the process to obtain the highest removal of Pb (II) (minimum final lead concentration), while the other input and output variables are set in range. Table 15 shows the results of the third adsorption scenario with the objective of achieving the minimum environmental impact and final Pb (II) concentration, with the remaining variables in range. The third scenario's output process parameter (minimum final lead concentration) and environmental effect were

considered in the fourth scenario (Table 16) in an attempt to minimize the activated carbon dosage consumption. After analyzing the results that appear in Table 16, we can conclude that the values for the input of dose of vine shoot activated carbon were very similar for each of the studied optimization scenarios, whereas the values for overall desirability were extremely close to -1-. This indicates that when starting with that given amount of vine shoot activated carbon, its saturation will be produced without implying greater adsorption during the process. Thus, the minimum value of the final Pb (II) concentration was achieved in the first ($C_F = 1.11$ ppm) and the second ($C_F = 1.12$ ppm) optimization scenarios, whereas the maximum final lead concentration was achieved in the fourth scenario ($C_F = 4.87$ ppm). Additionally, using Equation (6), the lead removal percentage for all of the optimization scenarios can be calculated. Therefore, the Pb (II) removal percentages that were achieved were 92.12% for the first optimization scenario, 92.09% for the second optimization scenario, 52.66% for the third optimization scenario, and 39.23% for the fourth optimization scenario. This indicates that the highest removal of Pb (II) ions was achieved in the first and second optimization scenarios, in which environmental impacts were not considered. Moreover, better results were obtained in this work than in studies undertaken by other researchers in the removal of lead with activated carbon derived from coconut shells [20] or residues of corn cobs [21]. The results that were obtained in this study are similar to those obtained with activated carbon from *Juniperus procera* leaves [47].

The values reached in the first two optimization scenarios for the input and output variables were identical. The values in the third and the fourth optimization scenarios were also identical. These last two scenarios were those that produced the least environmental impact. The first two optimization scenarios produced the optimal value of pH at 7 and an initial lead concentration (C_0) of 14.14 ppm when the dose of vine shoot activated carbon (dose) was 1.6 g, achieving a final lead concentration (C_F) of 1.11 ppm. The other values achieved were an environmental impact of 0.218 MJ for abiotic depletion (Ab_depl), 0.017 kg CO₂ eq. for global warming (Gl_War), 0.009 kg 1.4 DB eq. for human toxicity (Hum_Tox), 0.007 kg 1.4 DB eq. for freshwater ecotoxicity ($Fresh_W$), and 23.04 kg 1.4 DB eq. for marine aquatic ecotoxicity (Mar_Aqu). In the last two optimization scenarios, minimizing the environmental impact was an additional objective of the optimizations. For these scenarios, the optimal value of pH (pH) was 2.8, whereas the initial lead concentration (C_0) was 8.01 ppm and the dose of activated carbon (dose) was approximately 1.8 g, achieving a final lead concentration (C_F) of 3.8 and 4.87 ppm and an environmental impact of 0.047 MJ for abiotic depletion (Ab_depl), 0.004 kg CO₂ eq. for global warming (Gl_War), 0.002 kg 1.4 DB eq. for human toxicity (Hum_Tox), 0.001 kg 1.4 DB eq. for freshwater ecotoxicity ($Fresh_W$), and 4.86 kg 1.4 DB eq. for marine aquatic ecotoxicity (Mar_Aqu). There are two reasons why the highest lead removal values were reached in the first two optimization scenarios. The first is that, as the adsorbent surface charges, the pH of the solution determines the adsorbent's degree of ionization and specification. This factor greatly affects the number of heavy metal ions that are removed. Because lead precipitates in a solution at pH values higher than 6, lead adsorption is a process that is highly pH-dependent. The second reason is that the chemical structure of heavy metal ions often has a significant effect on the pH effect [53]. However, a greater lead initial concentration increases the adsorption capacity. As the process continues, the higher Pb (II) ion concentration must contend with a finite number of active sites on the vine shoot activated carbon surface. As a result, more Pb (II) ions remain in the solution and are not adsorbed.

Figure 3 is a 3D graphic representation of C_F vs. pH and C_0 , for the maximum (6 g) and minimum (1.6 g) values of vine shoot activated carbon dose. The figure indicates that, when the pH values are less than the study range ($pH = 2.8$), the C_F values that are achieved are always less. When the adsorbent dose is greater than any value of the C_0 study range, and when the pH values are the largest of the study range ($pH = 7.2$), the C_F values achieved are always less when the adsorbent dose is less than any value of the C_0 study range. Starting from the results shown, it can be confirmed that, if one intends to eliminate

the greatest possible quantity of Pb at the same time that the dose of adsorbent is the minimum possible, the pH of the water solution should have the maximum value of the study. Additionally, it can be deduced from Figure 3 that, when the pH is intermediate in the study range (from 4 to 6), the C_f values vary only in the study range of vine shoot activated carbon dose.

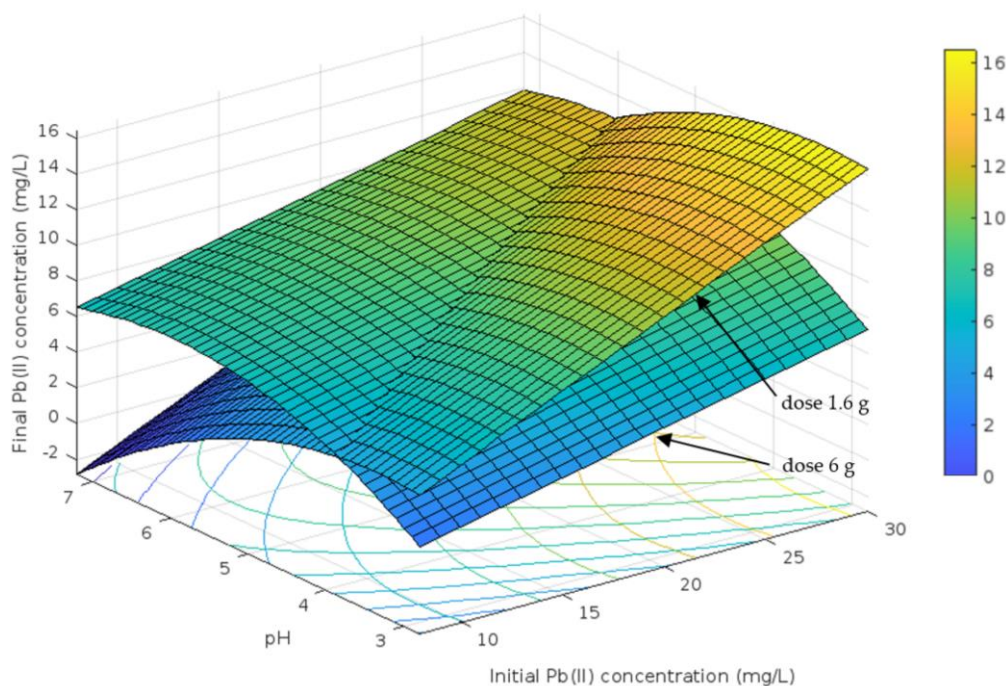


Figure 3. Graphic representation in 3D of C_f as a function of the pH and the C_0 for the maximum (6 g) and minimum (1.6 g) values of vine shoot activated carbon doses.

3.4. SEM-EDX Analysis

To ensure that the vine shoot activated carbon that had been used as an adsorbent contained lead, the samples were subjected to atomic adsorption spectroscopy. In this instance, raw vine shoot activated carbon (the sample not previously employed as an adsorbent) and the used vine shoot activated carbon (the sample used in the first optimization scenario) samples were compared.

The highest percentage of lead removal was achieved in the first optimization scenario (92.12%). Therefore, the activated carbon used in this scenario was analyzed using SEM. Figure 4 shows the ability of the activated carbon to hold onto Pb (II) ions. Figure 4a shows the vine shoot activated carbon surface morphology before the adsorption process, and Figure 4b shows the vine shoot activated carbon surface morphology after the adsorption process, where the Pb (II) ions that are trapped in the activated carbon can be seen in blue.

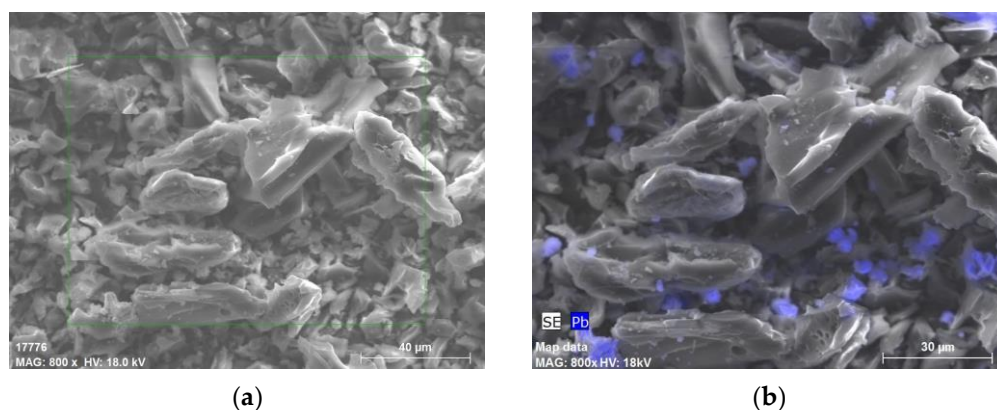


Figure 4. SEM image of activated carbon: (a) before Pb (II) ion adsorption; (b) after Pb (II) adsorption. Visible lead appears in blue.

Figure 5 shows EDX spectra of vine shoot activated carbon after the biosorption process in order to determine the constituent elements. It also provides a spectral analysis. This ensures that, in addition to being composed of its regular carbon and oxygen elements, Pb (II) ions have been adsorbed. The values for Au and Pd are due to the layer of gold–palladium that was deposited by plasma sputtering for SEM-EDX analysis.

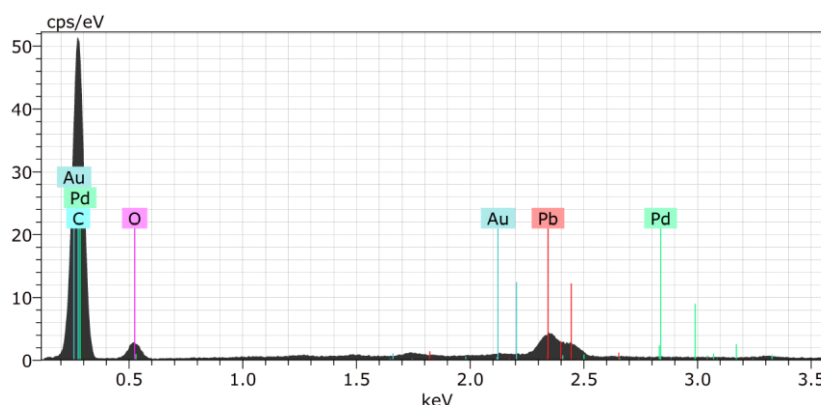


Figure 5. EDX spectra of vine shoot activated carbon.

4. Conclusions

It is a challenging task to determine the amount of adsorbent needed to remove Pb (II) ions from wastewater. The objective of this work was to conduct a thorough optimization, while investigating the use of vine shoot activated carbon as a low-cost biosorbent for Pb (II) removal from industrial wastewater, while attempting to reduce the negative effects of the process on the environment. This study combined the input and output parameters of four different optimization scenarios in an attempt to minimize the final lead ion concentration in wastewater, the adsorbent dosage consumption, and the environmental impact of the adsorption process. The percentage of Pb (II) removed was 92.12% for the first optimization scenario; this scenario sought to obtain the lowest final lead concentration. The percentage of Pb (II) removed was 92.09% for the second optimization scenario, which involved the minimum vine shoot activated carbon dosage consumption (thus minimizing the process costs) to obtain the highest removal of Pb (II). The percentage of Pb (II) removed was 52.66% for the third optimization scenario, which sought to produce the lowest impact on the environment and the lowest final Pb (II) concentration. The fourth scenario produced the worst elimination of Pb (II) ions (39.23%). It attempted to generate the lowest impact on the environment by minimizing the final Pb (II) concentration and vine shoot activated carbon dosage consumption. The highest removal of Pb (II) ions was achieved in the first and second optimization scenarios. The study also

showed how life cycle approaches can be used to assess the economic costs and environmental impact of implementing the optimal conditions generated by the RSM design. Overall, vine shoot activated carbon is a highly useful activated carbon for removing Pb (II) ions from water waste in a secure, sustainable, and cost-effective manner. In order to more fully understand the environmental effect of the process that is caused by the adsorption of heavy metals, a future study from an approach of cradle-to-gate or cradle-to-grave would be helpful. Furthermore, the use of other biosorbents or more input variables, such as reaction temperature, stirring speed, stirring time, or power consumption, would be of interest for a similar study.

Author Contributions: Conceptualization, M.C.-B.; data curation, R.L.-L. and F.S.-G.; formal analysis, C.S.-F.; investigation, C.S.-F., M.C.-B. and F.S.-G.; methodology, C.S.-F. and R.L.-L.; software, R.L.-L.; writing—original draft, C.S.-F. and F.S.-G.; writing—review and editing, M.C.-B. All authors have read and agreed to the published version of the manuscript.

Funding: This work was funded by the Government of La Rioja project ADER 2019-I-IDD-00047, which is partly funded by the European Regional Development Fund (ERDF).

Conflicts of Interest: The authors declare no conflict of interest.

References

1. Cheng, S.Y.; Show, P.-L.; Lau, B.F.; Chang, J.-S.; Ling, T.C. New Prospects for Modified Algae in Heavy Metal Adsorption. *Trends Biotechnol.* **2019**, *37*, 1255–1268. <https://doi.org/10.1016/j.tibtech.2019.04.007>.
2. Kumar, A.; Kumar, A.; Mms, C.-P.; Chaturvedi, A.K.; Shabnam, A.A.; Subrahmanyam, G.; Mondal, R.; Gupta, D.K.; Malyan, S.K.; Kumar, S.S. Lead Toxicity: Health Hazards, Influence on Food Chain, and Sustainable Remediation Approaches. *Int. J. Environ. Res. Public Health* **2020**, *17*, 2179.
3. Gutwiński, P.; Cema, G.; Ziemińska-Buczyńska, A.; Wyszynska, K.; Surmacz-Górska, J. Long-Term Effect of Heavy Metals Cr(III), Zn(II), Cd(II), Cu(II), Ni(II), Pb(II) on the Anammox Process Performance. *J. Water Process Eng.* **2021**, *39*, 101668. <https://doi.org/10.1016/j.jwpe.2020.101668>.
4. Debnath, B.; Singh, W.S.; Manna, K. Sources and Toxicological Effects of Lead on Human Health. *Indian J. Med. Spec.* **2019**, *10*, 66. https://doi.org/10.4103/INJMS.INJMS_30_18.
5. Bashir, A.; Malik, L.A.; Ahad, S.; Manzoor, T.; Bhat, M.A.; Dar, G.N.; Pandith, A.H. Removal of Heavy Metal Ions from Aqueous System by Ion-Exchange and Biosorption Methods. *Environ. Chem. Lett.* **2019**, *17*, 729–754. <https://doi.org/10.1007/s10311-018-00828-y>.
6. Chitpong, N.; Husson, S.M. High-Capacity, Nanofiber-Based Ion-Exchange Membranes for the Selective Recovery of Heavy Metals from Impaired Waters. *Sep. Purif. Technol.* **2017**, *179*, 94–103. <https://doi.org/10.1016/j.seppur.2017.02.009>.
7. Huang, Y.; Wu, D.; Wang, X.; Huang, W.; Lawless, D.; Feng, X. Removal of Heavy Metals from Water Using Polyvinylamine by Polymer-Enhanced Ultrafiltration and Flocculation. *Sep. Purif. Technol.* **2016**, *158*, 124–136. <https://doi.org/10.1016/j.seppur.2015.12.008>.
8. Lam, B.; Déon, S.; Morin-Crini, N.; Crini, G.; Fievet, P. Polymer-Enhanced Ultrafiltration for Heavy Metal Removal: Influence of Chitosan and Carboxymethyl Cellulose on Filtration Performances. *J. Clean. Prod.* **2018**, *171*, 927–933. <https://doi.org/10.1016/j.jclepro.2017.10.090>.
9. Azimi, A.; Azari, A.; Rezakazemi, M.; Ansarpour, M. Removal of Heavy Metals from Industrial Wastewaters: A Review. *Chem-BioEng Rev.* **2017**, *4*, 37–59. <https://doi.org/10.1002/cben.201600010>.
10. Zhou, G.; Luo, J.; Liu, C.; Chu, L.; Crittenden, J. Efficient Heavy Metal Removal from Industrial Melting Effluent Using Fixed-Bed Process Based on Porous Hydrogel Adsorbents. *Water Res.* **2018**, *131*, 246–254. <https://doi.org/10.1016/j.watres.2017.12.067>.
11. Zhou, G.; Luo, J.; Liu, C.; Chu, L.; Ma, J.; Tang, Y.; Zeng, Z.; Luo, S. A Highly Efficient Polyampholyte Hydrogel Sorbent Based Fixed-Bed Process for Heavy Metal Removal in Actual Industrial Effluent. *Water Res.* **2016**, *89*, 151–160. <https://doi.org/10.1016/j.watres.2015.11.053>.
12. Verma, B.; Balomajumder, C.; Sabapathy, M.; Gumfekar, S.P. Pressure-Driven Membrane Process: A Review of Advanced Technique for Heavy Metals Remediation. *Processes* **2021**, *9*, 752. <https://doi.org/10.3390/pr9050752>.
13. Shrestha, R.; Ban, S.; Devkota, S.; Sharma, S.; Joshi, R.; Tiwari, A.P.; Kim, H.Y.; Joshi, M.K. Technological Trends in Heavy Metals Removal from Industrial Wastewater: A Review. *J. Environ. Chem. Eng.* **2021**, *9*, 105688. <https://doi.org/10.1016/j.jece.2021.105688>.
14. Almomani, F.; Bhosale, R.; Khraisheh, M.; Kumar, A.; Almomani, T. Heavy Metal Ions Removal from Industrial Wastewater Using Magnetic Nanoparticles (MNP). *Appl. Surf. Sci.* **2020**, *506*, 144924. <https://doi.org/10.1016/j.apsusc.2019.144924>.
15. Chai, W.S.; Cheun, J.Y.; Kumar, P.S.; Mubashir, M.; Majeed, Z.; Banat, F.; Ho, S.-H.; Show, P.L. A Review on Conventional and Novel Materials towards Heavy Metal Adsorption in Wastewater Treatment Application. *J. Clean. Prod.* **2021**, *296*, 126589. <https://doi.org/10.1016/j.jclepro.2021.126589>.

16. Duan, C.; Ma, T.; Wang, J.; Zhou, Y. Removal of Heavy Metals from Aqueous Solution Using Carbon-Based Adsorbents: A Review. *J. Water Process Eng.* **2020**, *37*, 101339. <https://doi.org/10.1016/j.jwpe.2020.101339>.
17. Alghamdi, A.A.; Al-Odayni, A.-B.; Saeed, W.S.; Al-Kahtani, A.; Alharthi, F.A.; Aouak, T. Efficient Adsorption of Lead (II) from Aqueous Phase Solutions Using Polypyrrole-Based Activated Carbon. *Materials* **2019**, *12*, 2020. <https://doi.org/10.3390/ma12122020>.
18. Spigno, G.; Marinoni, L.; Garrido, G.D. 1—State of the Art in Grape Processing By-Products. In *Handbook of Grape Processing By-Products*; Galanakis, C.M., Ed.; Academic Press: Cambridge, MA, USA, 2017; pp. 1–27, ISBN 978-0-12-809870-7.
19. Dhahri, R.; Yilmaz, M.; Mechi, L.; Alsukaibi, A.K.D.; Alimi, F.; ben Salem, R.; Moussaoui, Y. Optimization of the Preparation of Activated Carbon from Prickly Pear Seed Cake for the Removal of Lead and Cadmium Ions from Aqueous Solution. *Sustainability* **2022**, *14*, 3245. <https://doi.org/10.3390/su14063245>.
20. Ramutshatsha-Makhwedzha, D.; Mbaya, R.; Mavhungu, M.L. Application of Activated Carbon Banana Peel Coated with Al₂O₃-Chitosan for the Adsorptive Removal of Lead and Cadmium from Wastewater. *Materials* **2022**, *15*, 860. <https://doi.org/10.3390/ma15030860>.
21. Jaber, L.; Ihsanullah, I.; Almanassra, I.W.; Backer, S.N.; Abushawish, A.; Khalil, A.K.A.; Alawadhi, H.; Shanableh, A.; Atieh, M.A. Adsorptive Removal of Lead and Chromate Ions from Water by Using Iron-Doped Granular Activated Carbon Obtained from Coconut Shells. *Sustainability* **2022**, *14*, 10877. <https://doi.org/10.3390/su141710877>.
22. Arul, A.; Kavitha, S.; Babu, A.A.; Surya, V.J.; Ravikumar, A.; Sivalingam, Y. Enhanced Removal of Pb (II) and Cd (II) Ions from Aqueous Systems Using Coated Magnetic Nanoparticles in Activated Carbon Derived from Corn cob Waste. *Surf. Interfaces* **2023**, 103095. <https://doi.org/10.1016/j.surfin.2023.103095>.
23. Teymur, Y.A.; Güzel, F. Ultra-Efficient Removal of Methylene Blue, Oxytetracycline, and Lead(II) by Activated Carbon Derived from Black Cumin (*Nigella Sativa*) Processing Solid Waste. *J. Water Process Eng.* **2023**, *54*, 103940. <https://doi.org/10.1016/j.jwpe.2023.103940>.
24. Myers, R.H.; Montgomery, D.C.; Anderson-Cook, C.M. *Response Surface Methodology: Process and Product Optimization Using Designed Experiments*; John Wiley & Sons: Hoboken, NJ, USA, 2016; ISBN 978-1-118-91603-2.
25. Moni, S.M.; Mahmud, R.; High, K.; Carbajales-Dale, M. Life Cycle Assessment of Emerging Technologies: A Review. *J. Ind. Ecol.* **2020**, *24*, 52–63. <https://doi.org/10.1111/jiec.12965>.
26. Rahman, S.M.; Eckelman, M.J.; Onnis-Hayden, A.; Gu, A.Z. Comparative Life Cycle Assessment of Advanced Wastewater Treatment Processes for Removal of Chemicals of Emerging Concern. *Environ. Sci. Technol.* **2018**, *52*, 11346–11358. <https://doi.org/10.1021/acs.est.8b00036>.
27. Pesqueira, J.F.J.R.; Pereira, M.F.R.; Silva, A.M.T. Environmental Impact Assessment of Advanced Urban Wastewater Treatment Technologies for the Removal of Priority Substances and Contaminants of Emerging Concern: A Review. *J. Clean. Prod.* **2020**, *261*, 121078. <https://doi.org/10.1016/j.jclepro.2020.121078>.
28. Li, Y.; Zhang, S.; Zhang, W.; Xiong, W.; Ye, Q.; Hou, X.; Wang, C.; Wang, P. Life Cycle Assessment of Advanced Wastewater Treatment Processes: Involving 126 Pharmaceuticals and Personal Care Products in Life Cycle Inventory. *J. Environ. Manag.* **2019**, *238*, 442–450. <https://doi.org/10.1016/j.jenvman.2019.01.118>.
29. Zepon Tarpani, R.R.; Azapagic, A. Life Cycle Environmental Impacts of Advanced Wastewater Treatment Techniques for Removal of Pharmaceuticals and Personal Care Products (PPCPs). *J. Environ. Manag.* **2018**, *215*, 258–272. <https://doi.org/10.1016/j.jenvman.2018.03.047>.
30. Kuroki, A.; Hiroto, M.; Urushihara, Y.; Horikawa, T.; Sotowa, K.-I.; Alcántara Avila, J.R. Adsorption Mechanism of Metal Ions on Activated Carbon. *Adsorption* **2019**, *25*, 1251–1258. <https://doi.org/10.1007/s10450-019-00069-7>.
31. Burakov, A.E.; Galunin, E.V.; Burakova, I.V.; Kucherova, A.E.; Agarwal, S.; Tkachev, A.G.; Gupta, V.K. Adsorption of Heavy Metals on Conventional and Nanostructured Materials for Wastewater Treatment Purposes: A Review. *Ecotoxicol. Environ. Saf.* **2018**, *148*, 702–712. <https://doi.org/10.1016/j.ecoenv.2017.11.034>.
32. Standard Test Methods for PH of Water. Available online: <https://www.astm.org/d1293-18.html> (accessed on 1 January 2023).
33. Box, G.E.P.; Wilson, K.B. On the Experimental Attainment of Optimum Conditions. In *Breakthroughs in Statistics: Methodology and Distribution*; Kotz, S., Johnson, N.L., Eds.; Springer Series in Statistics; Springer: New York, NY, USA, 1992; Volume 13, pp. 1–45, ISBN 978-1-4612-4380-9.
34. Corral Bobadilla, M.; Lostado Lorza, R.; Somovilla Gómez, F.; Escribano García, R. Adsorptive of Nickel in Wastewater by Olive Stone Waste: Optimization through Multi-Response Surface Methodology Using Desirability Functions. *Water* **2020**, *12*, 1320. <https://doi.org/10.3390/w12051320>.
35. Corral-Bobadilla, M.; Lostado-Lorza, R.; Somovilla-Gómez, F.; Escribano-García, R. Effective Use of Activated Carbon from Olive Stone Waste in the Biosorption Removal of Fe(III) Ions from Aqueous Solutions. *J. Clean. Prod.* **2021**, *294*, 126332. <https://doi.org/10.1016/j.jclepro.2021.126332>.
36. Ferreira, S.L.C.; Bruns, R.E.; Ferreira, H.S.; Matos, G.D.; David, J.M.; Brandão, G.C.; da Silva, E.G.P.; Portugal, L.A.; dos Reis, P.S.; Souza, A.S.; et al. Box-Behnken Design: An Alternative for the Optimization of Analytical Methods. *Anal. Chim. Acta* **2007**, *597*, 179–186. <https://doi.org/10.1016/j.aca.2007.07.011>.
37. Harrington, E.C. The Desirability Function. *Ind. Qual. Control* **1965**, *21*, 494–498.
38. Max, K. Desirability Function Optimization and Ranking. Available online: <https://CRAN.R-project.org/package=desirability> (accessed on 17 November 2022).

39. Vera Candiotti, L.; De Zan, M.M.; Cámara, M.S.; Goicoechea, H.C. Experimental Design and Multiple Response Optimization. Using the Desirability Function in Analytical Methods Development. *Talanta* **2014**, *124*, 123–138. <https://doi.org/10.1016/j.talanta.2014.01.034>.
40. Montgomery, D.C. *Design and Analysis of Experiments*; John Wiley & Sons: Hoboken, NJ, USA, 2017; ISBN 978-1-119-11347-8.
41. R Core Team. *R: A Language and Environment for Statistical Computing*; R Core Team: Vienna, Austria, 2013.
42. ISO 14044:2006; Environmental Management—Life Cycle Assessment—Requirements and Guidelines. International Standard Organization: Geneva, Switzerland, 2006.
43. Althaus, H.-J.; Hischier, R.; Doka, G.; Bauer, C.; Dones, R.; Nemecek, T.; Hellweg, S.; Humbert, S.; Margni, M.; Koellner, T.; et al. *Implementation of Life Cycle Impact Assessment Methods Data V20 (2007) Ecoinvent Report No 3*; Ecoinvent Centre: Gallen, Switzerland, 2007; p. 151.
44. Guinée, J.B. *Handbook on Life Cycle Assessment: Operational Guide to the ISO Standards*; Springer Science & Business Media: New York, NY, USA, 2002; ISBN 978-1-4020-0228-1.
45. Stocker, T.F.; Qin, D.; Plattner, G.-K.; Tignor, M.; Allen, S.K.; Boschung, J.; Nauels, A.; Xia, Y.; Bex, V.; Midgley, P.M. (Eds.) *Climate Change 2013: The Physical Science Basis. Contribution of Working Group I to the Fifth Assessment Report of the Intergovernmental Panel on Climate Change*; Cambridge University Press: Cambridge, UK, 2014.
46. Rosenbaum, R.K.; Bachmann, T.M.; Gold, L.S.; Huijbregts, M.A.J.; Jolliet, O.; Juraske, R.; Koehler, A.; Larsen, H.F.; MacLeod, M.; Margni, M.; et al. USEtox—The UNEP-SETAC Toxicity Model: Recommended Characterisation Factors for Human Toxicity and Freshwater Ecotoxicity in Life Cycle Impact Assessment. *Int. J. Life Cycle Assess* **2008**, *13*, 532. <https://doi.org/10.1007/s11367-008-0038-4>.
47. Igos, E.; Mailler, R.; Guillosoy, R.; Rocher, V.; Gasperi, J. Life Cycle Assessment of Powder and Micro-Grain Activated Carbon in a Fluidized Bed to Remove Micropollutants from Wastewater and Their Comparison with Ozonation. *J. Clean. Prod.* **2021**, *287*, 125067. <https://doi.org/10.1016/j.jclepro.2020.125067>.
48. Ali, I.H.; Al Mesfer, M.K.; Khan, M.I.; Danish, M.; Alghamdi, M.M. Exploring Adsorption Process of Lead (II) and Chromium (VI) Ions from Aqueous Solutions on Acid Activated Carbon Prepared from Juniperus Procera Leaves. *Processes* **2019**, *7*, 217. <https://doi.org/10.3390/pr7040217>.
49. Hamzenejhad, R.; Sepehr, E.; Samadi, A.; Rasouli Sadaghiani, M.H.; Khodaverdiloo, H. Adsorption Characteristics of Lead (Pb) from Aqueous Solutions by Grape Pruning Residues and Their Biochar. *J. Water Soil Conserv.* **2020**, *27*, 213–228. <https://doi.org/10.22069/jwsc.2020.16743.3206>.
50. Çiftçi, H.; Çalışkan, Ç.E.; İçtüzzer, Y.; Arslanoğlu, H. Application of Activated Carbon Obtained from Waste Vine Shoots for Removal of Toxic Level Cu(II) and Pb(II) in Simulated Stomach Medium. *Biomass Conv. Bioref.* **2023**. <https://doi.org/10.1007/s13399-023-03774-0>.
51. Haydar, S.; Farooq, M.U.; Gull, S. Use of Grape Vine Bark as an Effective Biosorbent for the Removal of Heavy Metals (Copper and Lead) from Aqueous Solutions. *DWT* **2020**, *183*, 307–314. <https://doi.org/10.5004/dwt.2020.25215>.
52. Corral-Bobadilla, M.; Lostado-Lorza, R.; Somovilla-Gómez, F.; Iñiguez-Macedo, S. Life Cycle Assessment Multi-Objective Optimization for Eco-Efficient Biodiesel Production Using Waste Cooking Oil. *J. Clean. Prod.* **2022**, *359*, 132113. <https://doi.org/10.1016/j.jclepro.2022.132113>.
53. Abbaszadeh, S.; Wan Alwi, S.R.; Webb, C.; Ghasemi, N.; Muhamad, I.I. Treatment of Lead-Contaminated Water Using Activated Carbon Adsorbent from Locally Available Papaya Peel Biowaste. *J. Clean. Prod.* **2016**, *118*, 210–222. <https://doi.org/10.1016/j.jclepro.2016.01.054>.

Disclaimer/Publisher’s Note: The statements, opinions and data contained in all publications are solely those of the individual author(s) and contributor(s) and not of MDPI and/or the editor(s). MDPI and/or the editor(s) disclaim responsibility for any injury to people or property resulting from any ideas, methods, instructions or products referred to in the content.